Abrupt Change of Bandgap Energy in Quantum System of Nanolayer on Silicon Surface

Wei-Qi Huang (wqhuang@gzu.edu.cn)
Guizhou University
Shi-Rong Liu
Institute of Geochemistry, Chinese Academy of Sciences
Zi-Lin Wang
Hainan Normal University
Cui-Fen Chen
Hainan Normal University
Ke Wang
Hainan Normal University
Hong-Yan Peng
Hainan Normal University
Zhong-Mei Huang
Guizhou University
An-Chen Wang
Guizhou University
Xin Li
Guizhou University

Nano Express

Keywords: Silicon nanolayer, abrupt change effect, quantum confinement, bandgap, simulated calculation

Posted Date: December 29th, 2020

DOI: https://doi.org/10.21203/rs.3.rs-135779/v1

Abstract

In the quantum system of nanolayer (NL) on silicon, the bandgap energy obviously increases with decreasing thickness of NL, in which the quantum confinement (QC) effect plays a main role. In simulating calculation, the QC effect has been exhibited as the thickness of Si NL changes along with (100), (110) and (111) direction respectively. And the simulation result demonstrated that the direct bandgap can be obtained as the NL with (001) direction is thinner than 10nm on Si surface. However, it is discovered in the simulated calculation that the QC effect disappears as the NL thickness arrives at size of monoatomic layer, in which its bandgap sharply deceases, where the abrupt change effect in bandgap energy occurs near idea 2D-layer. In experiment, we fabricated the Si NL structure by using electron beam irradiation and pulsed laser deposition methods, in which a novel way was used to control the NL thickness by modulating irradiation time of electron beam. The new effect should have a good application on optic-electronic chip of silicon.

Introduction

The nanostructures have been studied, mainly involving nanoparticle, nanowire and nanolayer in the past decade [1-5]. Especially, scientists have made an attention to the nanolayer (NL) structure due to its unique properties and applications [6–13]. Recently, in the quantum system of Si NL, some interesting phenomena and new effects have been discovered. In last few years, scientists have invested strong effort to growth of 2D silicon material [14, 15], which was expected to have a great impact on the development of future electronic devices and energy storage [16-18]. The molecular dynamics simulation was used to study the formation of double-layer silicon in slit pores, where their stability is further confirmed by first principles calculation in the simulated calculation [19, 20].

Here, it is interesting that the quantum confinement (QC) effect play a main role as the NL thickness is larger than 0.5nm. The energy bandgap obviously increases with decreasing thickness of NL by the QC effect in the quantum system of NL on silicon. In the article, the QC effect has been exhibited as the thickness of Si NL changes along with (100), (110) and (111) direction respectively in simulating calculation. And the simulation result demonstrated that the direct bandgap can be obtained as the NL diameter is smaller than 10nm in NL with (001) direction on Si surface. However, the bandgap energy of the NL changes in complicated ruler as the NL reaches to 2D Si material, where a new effect takes place on the energy change of NL bandgap. The bandgap energy in quantum system of NL on silicon surface abruptly changes as the NL is near 2D structure. It is discovered in the simulated calculation that the QC effect disappears as the NL thickness arrives at size of monoatomic layer, in which its bandgap energy sharply deceases where the abrupt change effect of bandgap energy occurs.

Fabrication of silicon nanolayer

Scientists usually used the self-assembly ways from silicon-rich silicon oxide matrices and plasma synthesis methods to fabricate various silicon nanostructures [21–27]. Here, the interesting method for

fabricating silicon nanocrystal is growth under laser photons interaction [28–30]. We have taken the interesting and simplest method for fabricating silicon nanolayer (NL), in which Si NL crystal rapidly grows with irradiation of electron beam on amorphous silicon film prepared by using pulsed laser deposition (PLD). The novel method of electron affection could be used to replace the traditional annealing methods in preparing process of silicon nanocrystals [31].

The coherent electron beam with 0.5 nA/nm^2 was used to irradiate on amorphous silicon film for 10-30min in Tecnai G2 F20 system, in which the electron beam from field-emission electron gun was accelerated by 200 KV and had higher energy and better coherent, where the silicon nanolayers with various thickness rapidly grew. The TEM image exhibits a geometry top viewed on the Si nanolayer as shown in Fig.1. Truly interesting, the several structures of silicene with quasi-2D film were obtained through controlling irradiation time and density of the coherent electron beam, which are respectively related to growing along with (100), (110) and (111) direction.

Investigation on Si nanolayer in simulation

The dynamic stability of the nanolayer was investigated by using first-principles calculations with consideration of three kinds of crystal structures observed in experiment, in which the crystal lattice grows respectively along with (100), (110) and (111) direction. The electronic behavior on the Si nanolayer was investigated by an ab initio nonrelativistic quantum mechanical analysis. The density functional theory (DFT) was used to calculate the density of states (DOS) on silicon nanolayers, which is carried out with the local density approximation (LDA) and gradient-corrected exchange-correlation function (GGA) for the self-consistent total energy methods.

It is interesting in the total energy calculations using DFT that the transformation from the indirect bandgap to direct bandgap can be obtained as the nanolayer thickness is smaller than 10nm, wholes simulated model of NL structure along with (001) direction and its direct bandgap are shown in Fig.2(a) and (b) after simulated calculation. It is originated from the Heisenberg principle related to $\Delta hK_x \geq h/\Delta x$, in which the wave vector will relax from X region to Γ region as the Δx decreases to nanoscale (relaxing relation: $\Delta x\downarrow \rightarrow \Delta K_x\uparrow$), where higher electronic speed is obtained in nanolayer.

In the experimental result, the nanolayer of silicon crystal growing along with (100) direction was prepared, as shown in Fig.3(a), where the TEM image exhibits its structure. In the simulated calculation, the DMol3 mode is used to make optimum atomic structure for obtaining the lowest combining energy, and the CASTEP mode is used to simulate for obtaining the energy band structure after optimum process. In Fig.3(b), the simulation model of the Si nanolayer has been built along with (100) direction according to the experimental result. After optimization process in simulation, the quasi-2D structure of silicon crystal with the rectangular lattice occurs in the lowest energy of optimum structure, as shown in Fig.3(c). The structural transformation from the ideal model of 2D structures to the optimal quasi-2D structures of Si crystal along with (100) direction should be noted in the simulation process, where the convex bonding angles take place on silicon film.

The Fig.3(d) exhibits the change curve of bandgap energy with various thicknesses of Si NL along with (100) direction in the simulation result, where it is interesting that the quantum confinement (QC) effect plays a main role as the nanolayer thickness is lager, but the QC effect disappears as the nanolayer thickness is smaller than 0.4nm near monoatomic layer, when its bandgap energy abruptly decreases. Truly interesting, the QC effect disappears as the nanolayer thickness reaches to size of monoatomic layer, where its bandgap sharply deceases. This abrupt change effect in bandgap energy may be originated from transforming between different dimensions at the symmetry broken point, in which the quasi-2D shape of NL is transformed to the two dimensional quantum layer. Here, the abrupt change effect in bandgap energy was observed and studied at first.

The nanolayer structure of the Si crystal growing along with (110) direction was obtained, as shown in the TEM image of Fig.4(a), from whom we can build the simulation model of the Si nanolayer in this direction, as exhibited in Fig.4(b). The idea model structure with the hexagonal lattice is transformed to the real quasi-2D structure with convex atomic bonds after simulated optimum process, as shown in Fig.4(c). In the same way, the abrupt change effect in bandgap energy takes place as the nanolayer thickness reaches to size of monoatomic layer, where the QC effect disappears, as shown in Fig.4(d). Here, it is interesting to make a compression between the quasi-2D silicene with the hexagonal lattice and the graphite. The simulation result demonstrates that the indirect bandgap can be transformed to the direct bandgap as the nanolayer thickness along with (110) direction is smaller than 3nm.

In the same way, the TEM image in Fig.5(a) shows the nanolayer structure of the Si crystal growing with (111) direction, according to whom the simulated model of the Si nanolayer in this direction can be built, as shown in Fig.5(b). The real quasi-2D structure along with Si crystal (111) direction can be obtained after simulated optimum process, as exhibited in Fig.5(c). The result of simulated calculation demonstrates that the QC effect plays a main role as the nanolayer thickness is larger, in which the indirect bandgap is almost kept in thickness changing. In the same manner, the abrupt change effect in bandgap energy was discovered in the simulated calculation, where the bandgap energy deeply decreases as the nanolayer thickness arrives near monoatomic layer, as shown in Fig.5(d). Here, it is should be noted that the bandgap rapidly disappears in the process.

The abrupt change effect in bandgap energy may be originated from transforming between different dimensions at the symmetry broken point. In the picture (c) of Fig.3, Fig.4 or Fig.5, the structure near monoatomic layer belongs to the fractional dimension of 2.1~2.5 in quasi-2D situation, and the bandgap will disappear to become a semi-metal, where new quantum phenomena and effects will appear in the process from the 3D layer to the quasi-2D shape and to the idea quantum surface.

Methods

Preparation of silicon nanolayers

Preparation of silicon nanolayers involves two steps: fabrication of Si amorphous nanolayer by using PLD process and growth of Si nanolayer by using electron beam irradiation. At first, a silicon wafer (100),

(110) or (111) oriented substrate was taken on the sample stage in the combination fabrication system with pulsed laser etching (PLE) and pulsed laser deposition (PLD) devices. A pulsed Nd:YAG laser (wavelength: 1064nm, pulse length: 60ns FWHM, repetition rate: 1200) was used to etch lines on Si substrate in PLE process. Then, a third harmonic of pulsed Nd:YAG laser at 355nm was used to deposit the silicon amorphous nanolayer in PLD process. And second, we accelerate the electron beam from field-emission electron gun by 200 KV and make it have higher energy and better coherent. The coherent electron beam with 0.5 nA/nm^2 was used to irradiate on amorphous Si nanolayer for 10-30min in Tecnai G2 F20 system, where the silicon nanolayers with various thickness rapidly grow, while the TEM images of nanolayers were taken at the same time. The thickness change of the Si NL can be controlled by modifying irradiation time and density of the coherent electron beam.

Transmission electron microscope (TEM) analysis

In the TEM (FEI Tecnai G2 F20) image, the various nanolayer structures of silicon are detected in vacuum (10^{-8} Pa), in which the electron beam from field-emission electron gun is accelerated by 200 KV, and the compositions are measured on the samples by using analysis in X-ray energy spectra.

Simulated calculation

First-principles total-energy calculations are used to optimize the equilibrium geometries and the relative energies of the simulation models on the silicon nanolayers. The simulated calculation is performed in the surface geometry with various nanolayer thickness along with the reconstructed top surface layer (100), (110) or (111), and vacuum region of at least 0.5nm. All atomic positions are relaxed, except the bottom Si layer and its passivating hydrogen layer. The electronic behavior is investigated by an ab initio non-relativistic quantum mechanical analysis in this work. Total energies and forces are calculated within the local density approximation (LDA) and generalized gradient approximation (GGA) for the self-consistent total energy methods to DFT, as implement in the CASTEP.

Conclusion

In summary, we have prepared the nanolayer structures on silicon in the experiment. In the simulated calculation, the change ruler of bandgap energy with nanolayer thickness has been explored, where the abrupt change effect in bandgap energy was discovered as the nanolayer thickness deceases to arrive near monoatomic layer, in which the Dirac-cone shape gradually occurs and the bandgap disappears in K space on quasi-2D silicene. The new effects will be explored deeply in the process from the 3D layer to the 2D structure of silicon. In the experiment, the thickness change can be controlled by manipulating irradiation time and density of the coherent electron beam, which will provide an investigation platform on quantum system of silicon. The results of experiment and calculation demonstrate that the transformation from the indirect bandgap to the direct bandgap can be obtained really in the nanolayer of silicon growing along with (100) direction as the thickness is smaller than 10nm, which has a good application on optic-electronic material and devices.

Declarations

Acknowledgment

This work was supported by the National Natural Science Foundation of China (Grant Nos. 11847084). This work was supported by Science Foundation of Guizhou (No.20185781) and Science Foundation of Guizhou university (Nos.2017(03), 20185781-17).

Author contributions

W.-Q.H. is the main writers and researchers, who wrote the main manuscript text and prepared Figures 1–5, provided new ideas and designed investigation plan in research. S.-R.L. is a main researcher in experimental work, who took part in preparing figures 1 and 2 and took part in measurement of TEM on the samples; Z.-L.W. is a main researcher in experimental work, taking part in preparing figures 2–4; C.-F.C. is a main researcher in experimental work, taking part in preparing figures 3 and 4; K.W. is a main researcher in experimental work, taking part in preparing figures 2 and 3; H.-Y. P. is a main researcher in experimental work, taking part in preparing figures 3 and 4; Z.-M.H. is a main researcher in investigation work, who is the main researchers in experimental work, took part in the preparing process of the samples, took part in preparing figures 3-5 and made spectra measurement on the samples; A.-C.W. is a main researcher in experimental work, taking part in preparing figures 4 and 5; X.L. is a main researcher in experimental work, taking part in preparing figures 3 and 4. All authors discussed the results and commented on the paper.

Competing financial interests

The authors declare no competing interests and financial interests.

References

1. Godefroo S,*et al.* (2008) Classification and control of the origin of photoluminescence from Si nanocrystals. *Nature Nanotech*. **3:** 174–178
2. Daldosso N, *et al.* (2003) Role of the interface region on the optoelectronic properties of silicon nanocrystals embedded in SiO2. *Phys.Rev. B* **68:** 085327
3. Wolkin M, Jorne J, Fauchet P, Allan G and Delerue C (1999) Electronic states and luminescence in porous silicon quantum dots: the role of oxygen. *Phys. Rev. Lett*. **82:** 197–200
4. Pavesi L and Turan R (Wiley-VCH, 2010) (eds) *Silicon Nanocrystals; Fundamentals, Synthesis, and Applications*
5. Koshida N (Springer, 2008) (ed.) *Nanostructure Science and Technology: Device Applications of Silicon Nanocrystals and Nanostructures*
6. Qian F, Gradecˇak S, Li Y, Wen C Y and Lieber C M (2005) Core/Multishell Nanowire Heterostructures as Multicolor, High-Efficiency Light-Emitting Diodes. (2018) Nano Lett. 5: 2287

7. ROUZBEH MOLAEI IMEN ABADI and MEHDI SAREMI, A Resonant Tunneling Nanowire Field Effect Transistor with Physical Contractions: A Negative Differential Resistance Device for Low Power Very Large Scale Integration Applications, Journal of Electronic Materials, 47: 1091-1098
8. Tomioka K, Motohisa J, Hara S, Hiruma K and Fukui T (2010) GaAs/AlGaAs Core Multishell Nanowire-Based Light-Emitting Diodes on Si. Nano Lett. 10: 1639
9. Mayer B, Rudolph D, Schnell J, Mork€otter S, Winner J, Treu J, M€uller K, Bracher G, Abstreiter G, Koblm€uller G and Finley J J (2013) Lasing from individual GaAs-AlGaAs core-shell nanowires up to room temperature. Nat. Commun.4: 2931
10. Saxena D, Mokkapati S, Parkinson P, Jiang N, Gao Q, Tan H H and Jagadish C (2013) Optically pumped room-temperature GaAs nanowire lasers. Nat. Photonics 7: 963
11. Bryllert T, Wernersson L E, Froberg L E and Samuelson L (2006) Vertical High-Mobility Wrap-Gated InAs Nanowire Transistor. IEEE ElectronDevice Lett. 27: 323
12. Tomioka K, Yoshimura M and Fukui T (2012) A III–V nanowire channel on silicon for high-performance vertical transistors. Nature 488: 189
13. Wallentin J,*et al.* (2013) InP Nanowire Array Solar Cells Achieving 13.8% Efficiency by Exceeding the Ray Optics Limit. Science 339: 1057
14. Feng B, *et al.* (2012) Evidence of Silicene in Honeycomb Structures of Silicon on Ag(111). *Nano Lett.* 12: 3507–3511
15. Lalmi B, *et al.* (2010) Epitaxial growth of a silicene sheet. *Appl. Phys. Lett.* 97: 223109
16. Takeda K and Shiraishi K (1994) Theoretical possibility of stage corrugation in Si and Ge analogs of graphite. *Phys. Rev. B* 50: 14916–14922
17. Guzmán-Verri G G and Lew Yan Voon L C (2007) Electronic structure of silicon-based nanostructures. *Phys. Rev. B* 76: 075131
18. Tsai W F, *et al.* (2012) Gated silicene as a tunable source of nearly 100% spin-polarized electrons, *Nat. Commun.* 4: 1500
19. Morishita T, Nishio K and Mikami M (2008) Formation of single- and double-layer silicon in slit pores. *Phys. Rev. B* 77: 081401(R)
20. Nishio K, Morishita T, Shinoda W and Mikami M (2006) Molecular dynamics simulations of self-organized polyicosahedral Si nanowire. *J. Chem. Phys.* 125: 074712
21. 21. Kanzawa Y, *et al.* (1997) Size-dependent near-infrared photoluminescence spectra of Si nanocrystals embedded in SiO2 matrix. *Solid State Commun.* **7:** 533–537
22. 22. Iacona F, Bongiorno C, Spinella C, Boninelli S and Priolo F (2004) Formation and evolution of luminescent Si nanoclusters produced by thermal annealing of SiO*x J. Appl. Phys.* **95:** 3723
23. 23. Zacharias M, *et al.* (2002) Size-controlled highly luminescent silicon nanocrystals: A SiO/SiO2 superlattice approach. *Phys. Lett.* **80:** 661–663
24. 24. Liu C Y, Holman Z C and Kortshagen U R L (2010) Optimization of Si NC/P3HT hybrid solar cells. *Funct. Mater.* **20:** 2157–2164

25. 25. Mangolini L, Thimsen E and Kortshagen U (2005) High-yield plasma synthesis of luminescent silicon nanocrystals. *Nano Lett.* **5:** 655–659
26. 26. Jurbergs D, Rogojina E, Mangolini L and Kortshagen U (2006) Silicon nanocrystals with ensemble quantum yields exceeding 60%. *Phys. Lett.* **88:** 233116
27. 27. Gupta A, Swihart M T and Wiggers H (2009) Luminescent colloidal dispersion of silicon quantum dots from microwave plasma synthesis: Exploring the photoluminescence behavior across the visible spectrum. *Funct. Mater.* **19:** 696–703
28. 28. Niesar S, *et al.* (2012) Low-cost post-growth treatments of crystalline silicon nanoparticles improving surface and electronic properties. *Funct. Mater.* **22:** 1190–1198
29. 29. Alima D, Estrin Y, Rich D H and Bar I (2012) The structural and optical properties of supercontinuum emitting Si nanocrystals prepared by laser ablation in water, *APPL. PHYS.* **112:** 114312
30. 30. Crouch C H, *et al.* (2004) Comparision of structure and properties of femtosecond and nanosecond laser-structured silicon, *Phys. Lett.* **84:** 1850–1852
31. Huang W Q, *et al.* (2015) Magic electron affection in preparation process of silicon nanocrystal, SCIENTIFIC REPORTS **4**: 9932

Figures

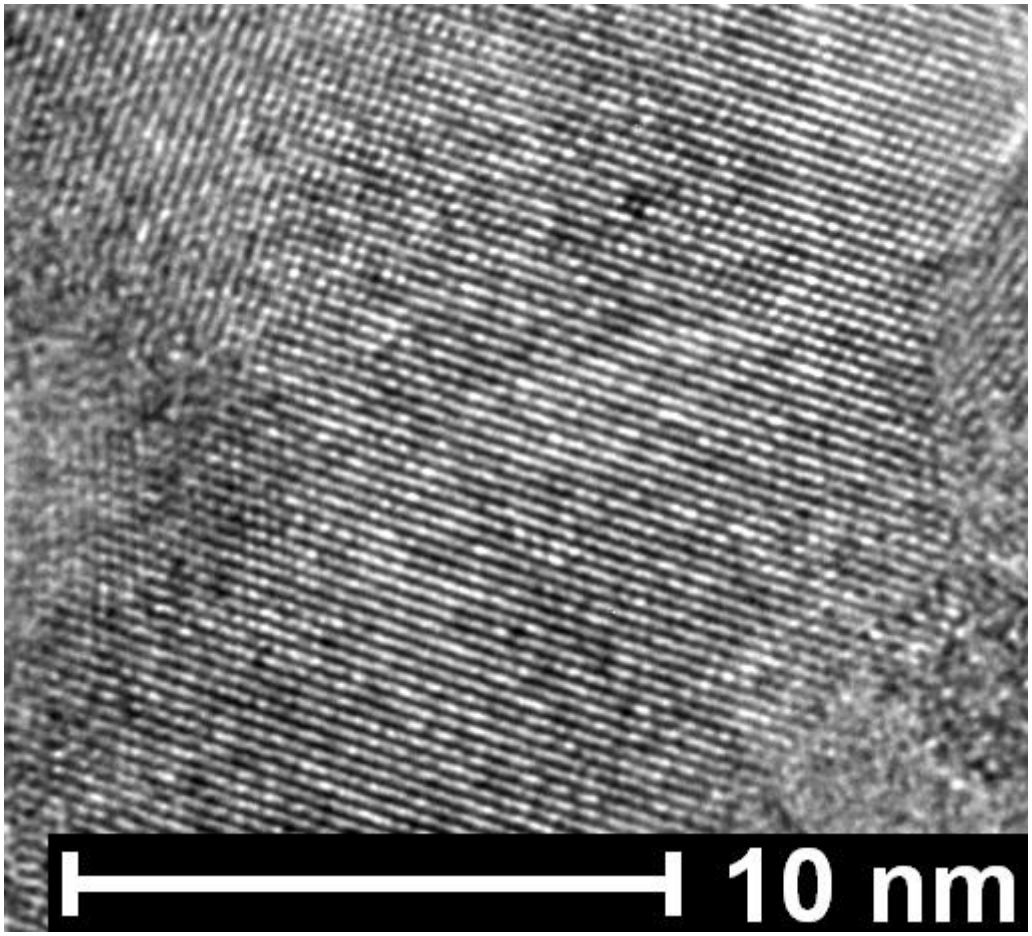

Figure 1

The TEM image exhibiting a geometry top viewed on the Si nanolayer

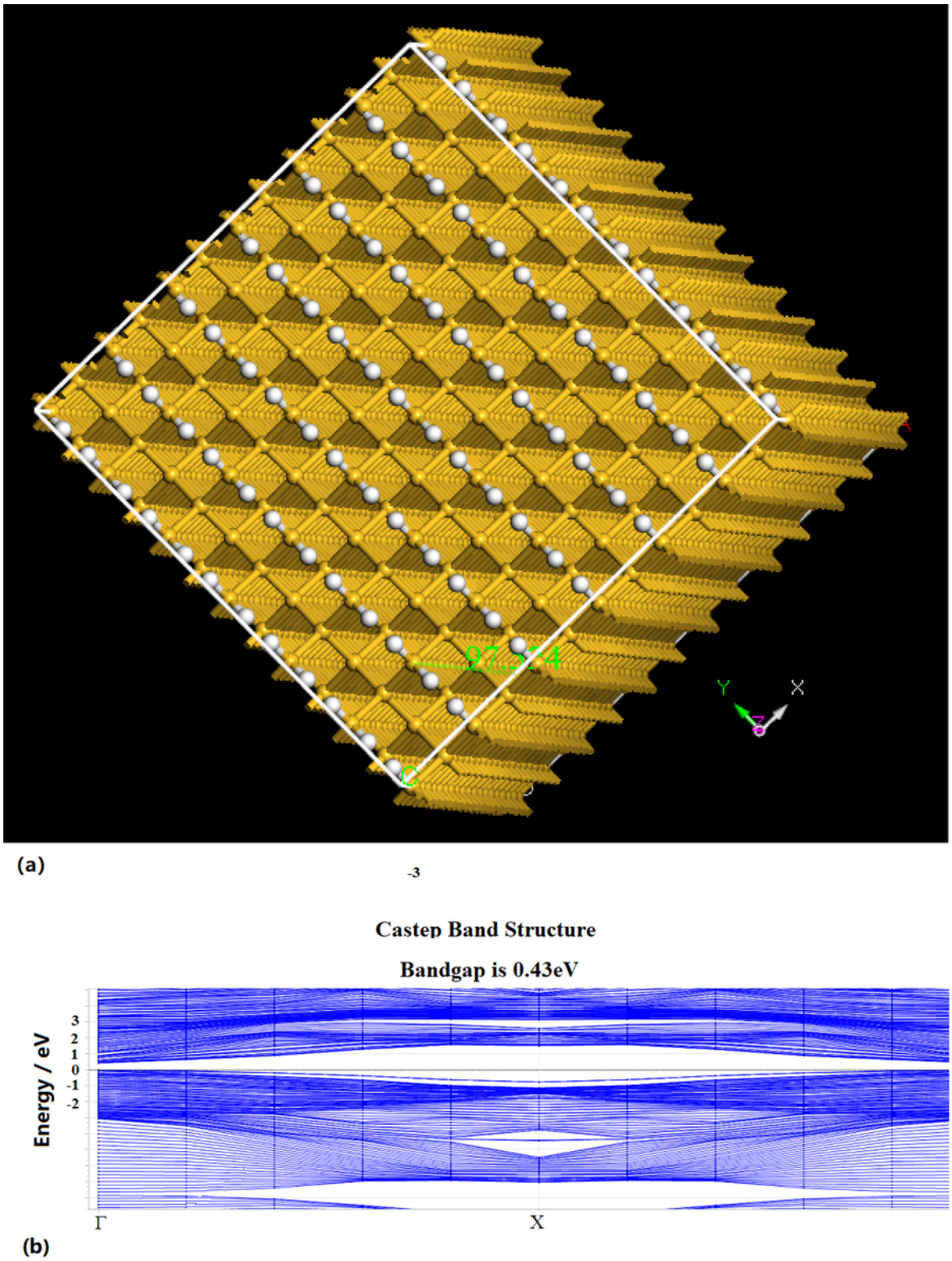

Figure 2

(a) The simulated model of NL structure along with (001) direction (b) The energy band construction of the NL structure along with (001) direction, in which the direct bandgap can be obtained

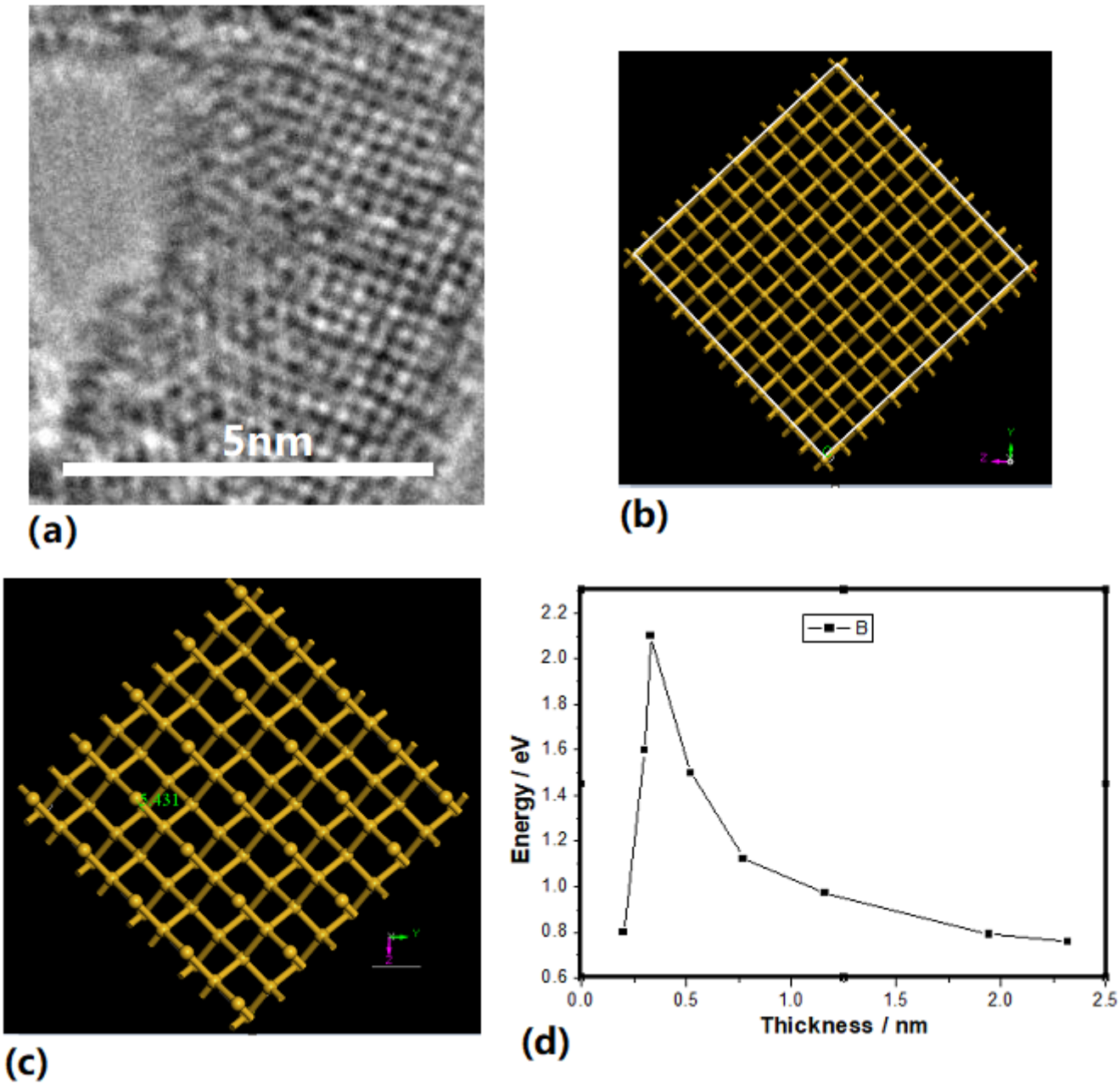

Figure 3

(a) TEM image of Si NL crystal growing along with (100) direction (b) The simulation model of the Si NL built along with (100) direction according to the experimental result (c) The quasi-2D structure of the Si NL crystal with the rectangular lattice occurring in the lowest energy of optimum structure after optimization process in simulation (d) The change curve of bandgap energy with various thicknesses of Si NL along with (100) direction in the simulation result

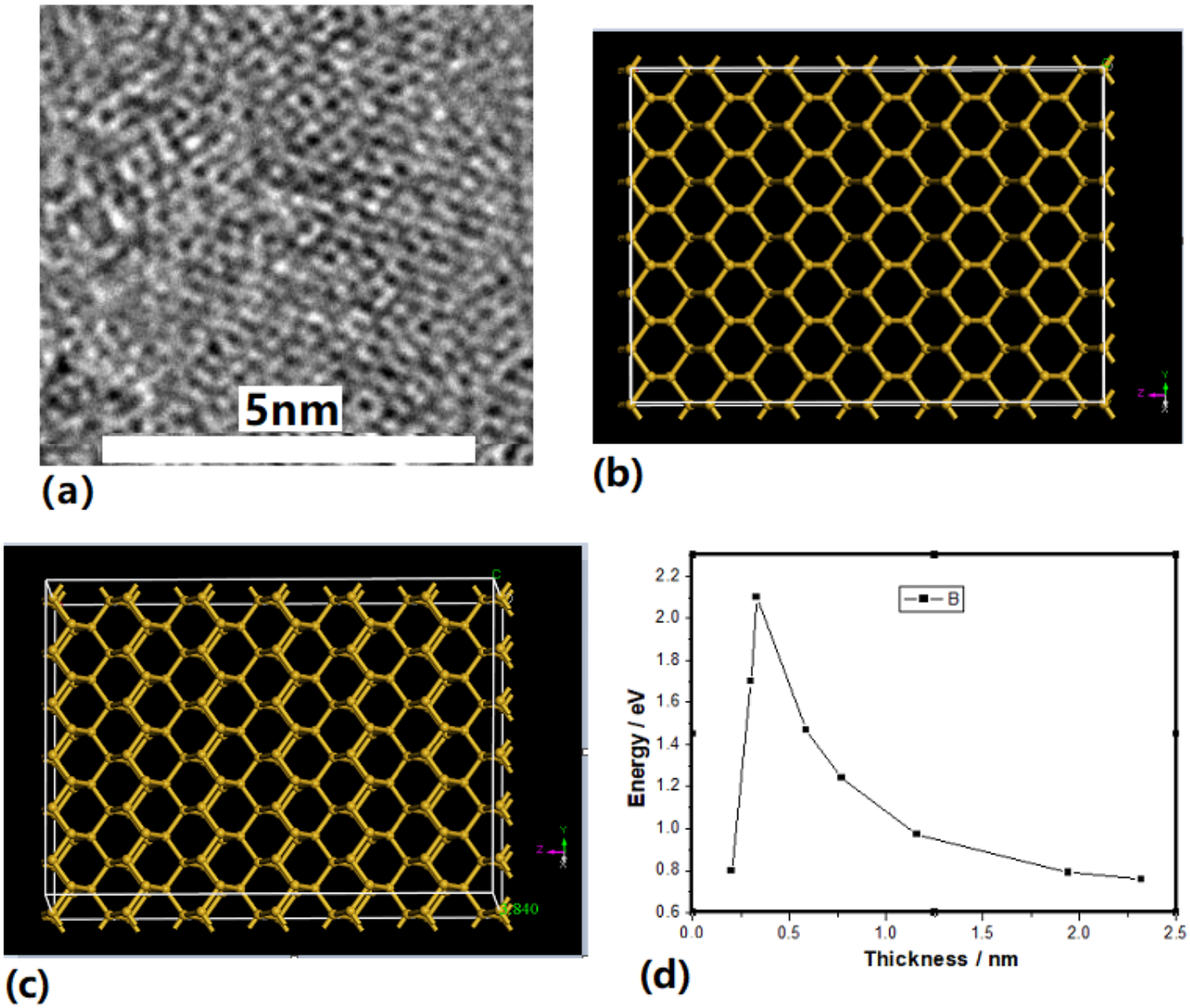

Figure 4

(a) TEM image of Si NL crystal growing along with (110) direction (b) The simulation model of the Si NL built along with (110) direction according to the experimental result (c) The quasi-2D structure of the Si NL crystal with the hexagonal lattice occurring in the lowest energy of optimum structure after optimization process in simulation (d) The change curve of bandgap energy with various thicknesses of Si NL along with (110) direction in the simulation result

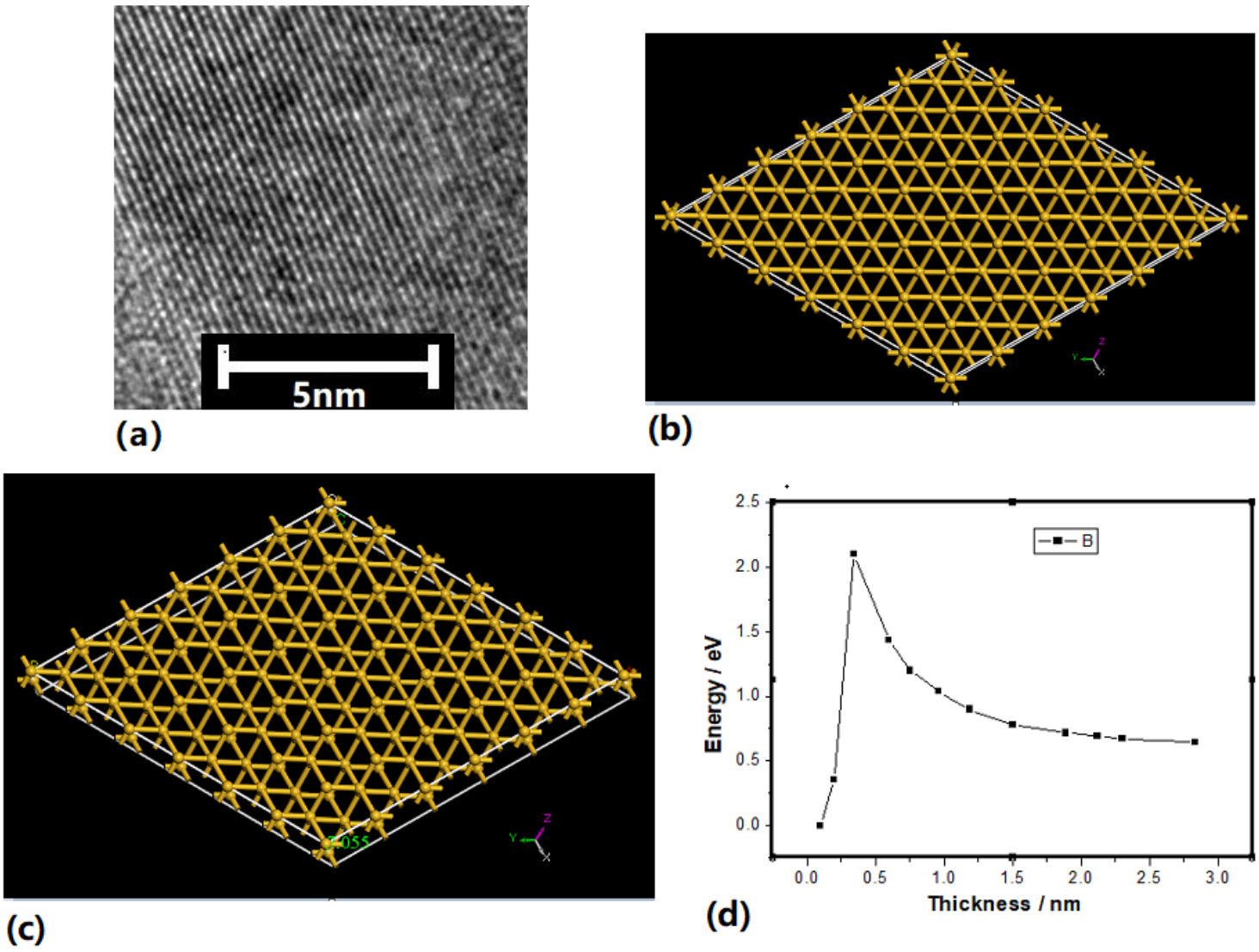

Figure 5

(a) TEM image of Si NL crystal growing along with (111) direction (b) The simulation model of the Si NL built along with (111) direction according to the experimental result (c) The quasi-2D structure of the Si NL crystal along with (111) direction occurring in the lowest energy of optimum structure after optimization process in simulation (d) The change curve of bandgap energy with various thicknesses of Si NL along with (111) direction in the simulation result